

Electronic Supplementary Information

A dual-emissive MOF for the simultaneous detection of tetrachlorobenzoquinone isomers in their mixtures

Xiao-Meng Du, Qian Wang, Qiao Liu, Di Ning, Bo Zhao, Yue Li* and Wen-Juan Ruan*

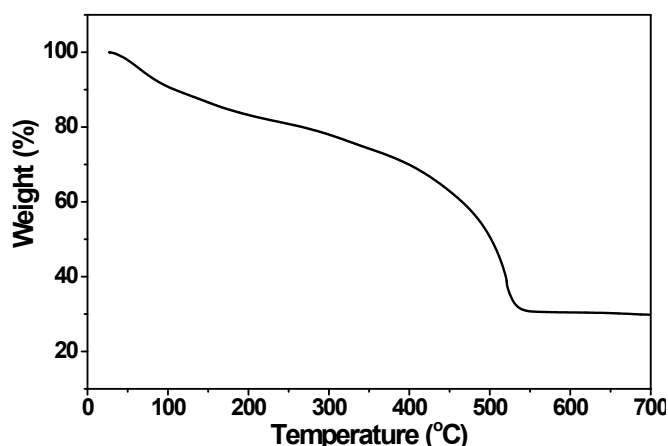


Fig. S1 Thermogravimetric curve of as-synthesized UiO-66-(COOH)₂ sample in air atmosphere. The overall weight loss from room temperature to 700 °C is 70.18%, which is in good consistency with the calculated value of 70.25% for the loss of all H₂O molecules, OH⁻ ions and organic components based on the formula of [Zr₆(O)₄(OH)₄(H₂btec)₆(H₂O)₁₆].

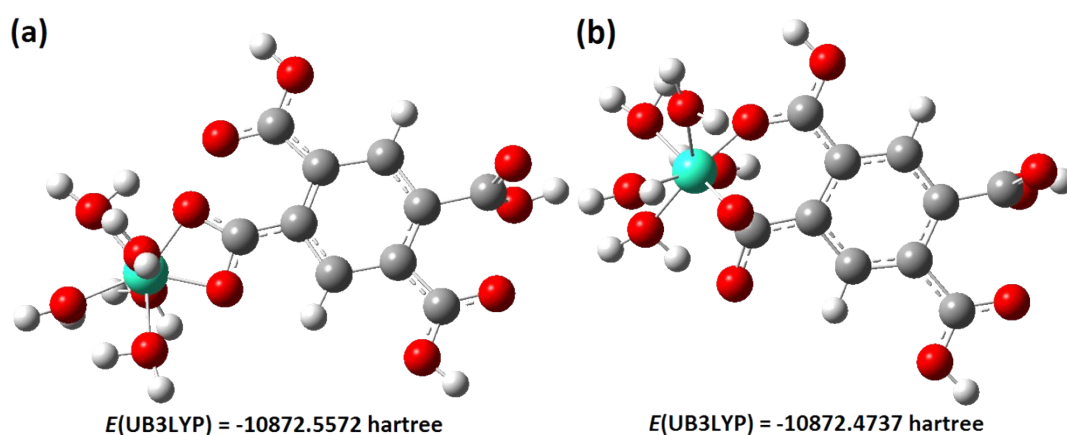


Fig. S2 Optimized structures of the coordination compounds formed between H₂btec²⁻ and Tb³⁺ ion with (a) one and (b) two carboxyl groups take part in coordination. Both the geometry optimization and single point energy calculation were performed using B3LYP functional and a mixed basis set of SDD for Tb and 6-31G(d) for other atoms. The solvent effect was modulated with SMD model (aqueous solvent). The sub-structure of terephthalate in the H₂btec²⁻ ligand was picked up from the crystalline structure of UiO-66, and protons were added to carboxylate groups for charge balance. Two carboxyl groups were added to the central benzene ring, and Tb atom was placed near one of them. five H₂O molecules were placed around Tb atom to keep the coordination saturation. During the optimization process, the atoms of the initial two carboxylate groups were fixed to replicate the bulk behavior, while the other atoms were relaxed.

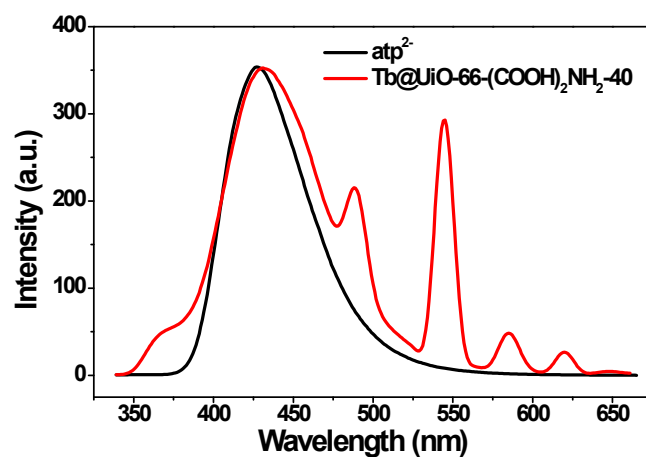


Fig. S3 Comparison between the photoluminescent spectra of Tb@UiO-66-(COOH)₂NH₂ (50 mg L⁻¹) and free atp²⁻ ligand (4 μM, dissolving H₂atp by 2 equiv of NaOH) in H₂O-ethanol mixed solvent (v/v = 3/1), λ_{ex} = 290 nm.

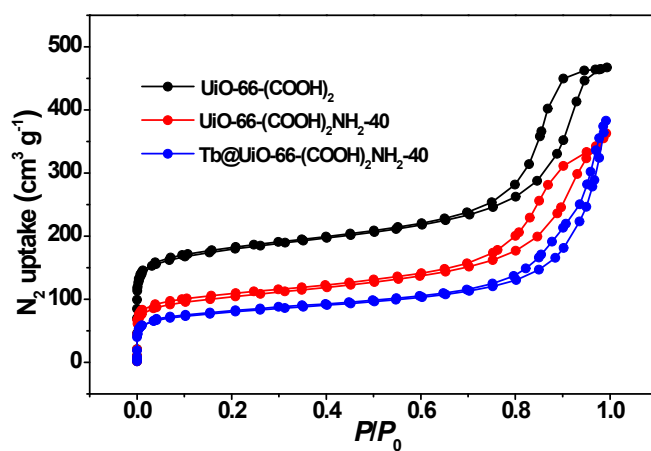


Fig. S4 N₂ adsorption isotherms (at 77 K) of UiO-66-(COOH)₂ precursor and its product after post-synthetic modification.

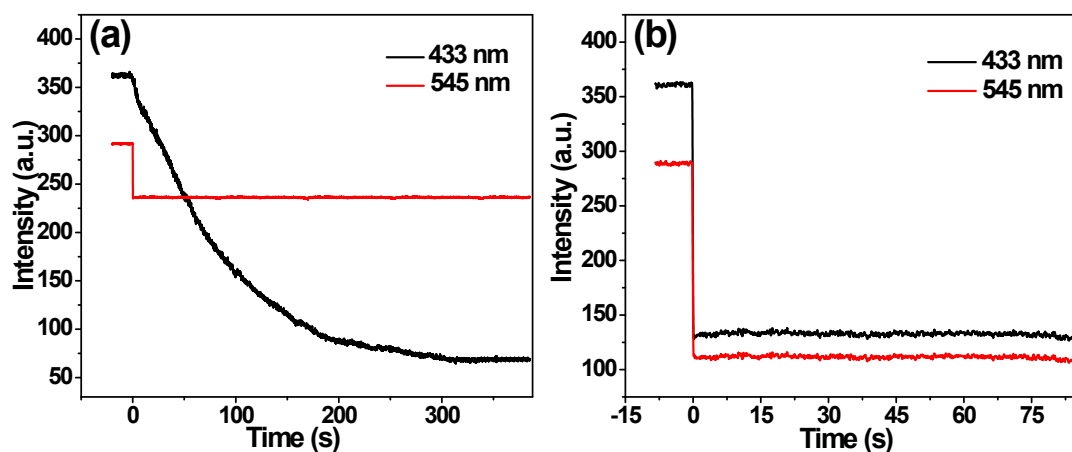


Fig. S5 Temporal fluorescent change of Tb@UiO-66-(COOH)₂NH₂-40 emission intensity upon the addition of (a) *o*-TCBQ (100 μM) and (b) *p*-TCBQ (100 μM). 50 mg L⁻¹ MOF, in H₂O-ethanol mixed solvent (*v/v* = 3/1), λ_{ex}=290 nm.

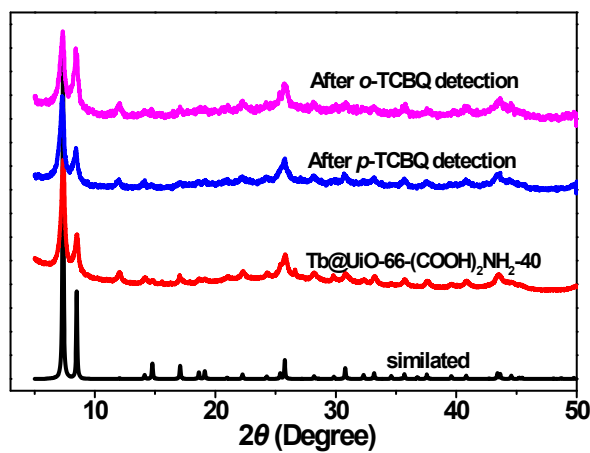


Fig. S6 Comparison among the PXRD patterns of Tb@UiO-66-(COOH)₂NH₂-40 before and after the detection of *o*- and *p*-TCBQs.

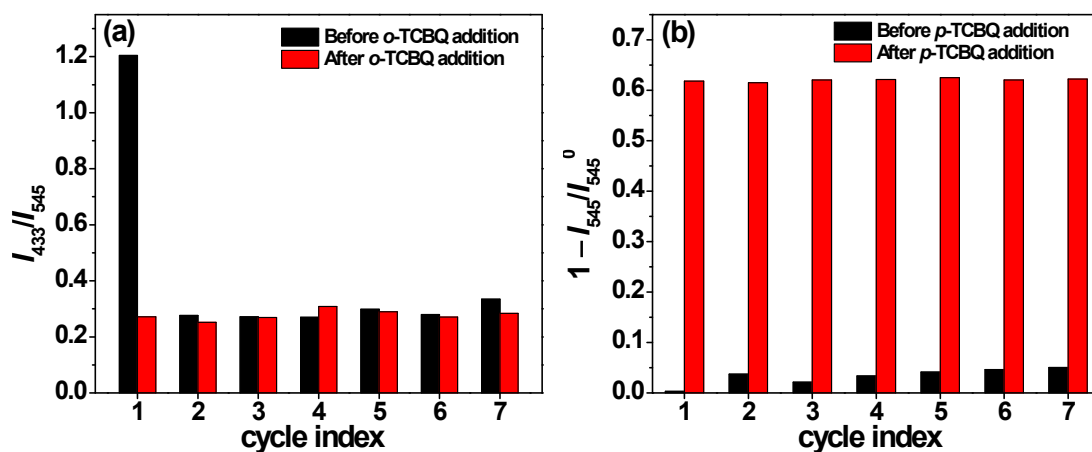


Fig. S7 Fluorescent signals of Tb@UiO-66-(COOH)₂NH₂-40 during 7 consecutive detection and generating cycles with the analyte of (a) *o*-TCBQ (100 μ M) and (b) *p*-TCBQ (100 μ M). 50 mg L⁻¹ MOF, in H₂O-ethanol mixed solvent (v/v = 3/1), λ_{ex} =290 nm.

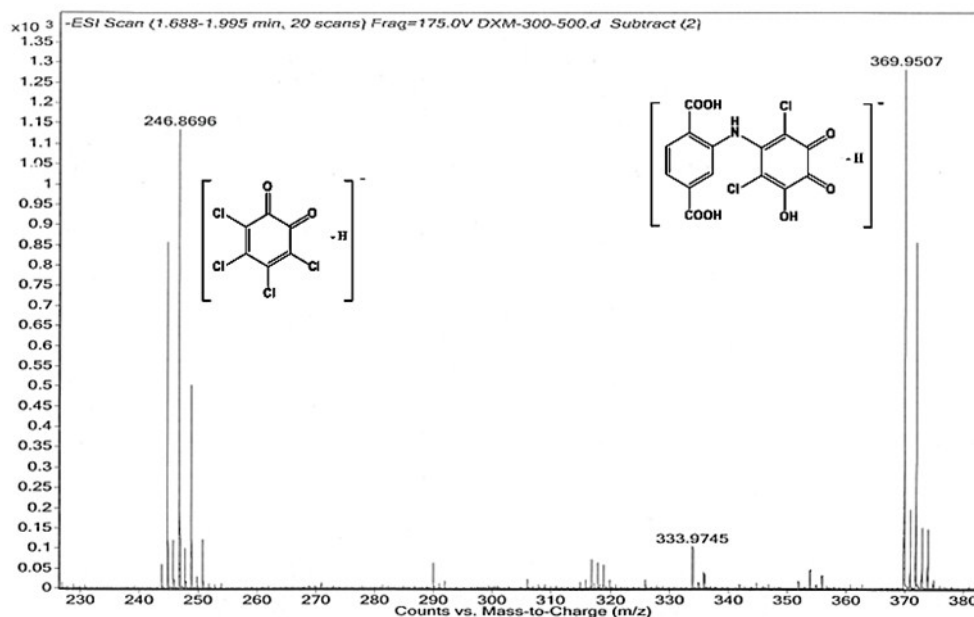


Fig. S8 ESI-MS (negative mode) of the digested solution of UiO-66-NH₂ after the treatment by *o*-TCBQ.

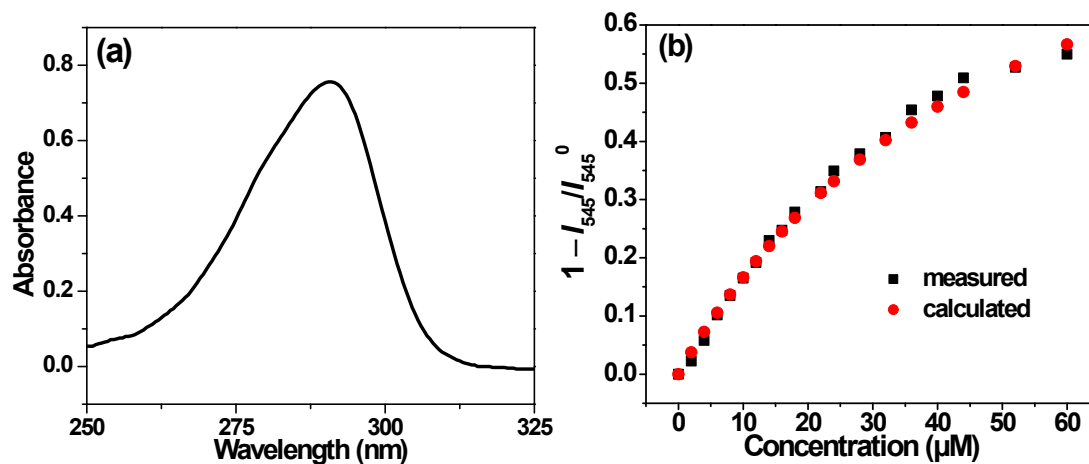


Fig. S9 (a) Absorption spectrum of *p*-TCBQ (50 μM). (b) Comparison between the calculated and measured quenching efficiency of Tb@UiO-66-(COOH)₂NH₂-40 (50 mg L⁻¹) upon the exposure to different concentrations of *p*-TCBQ, $\lambda_{\text{ex}}=290$ nm.

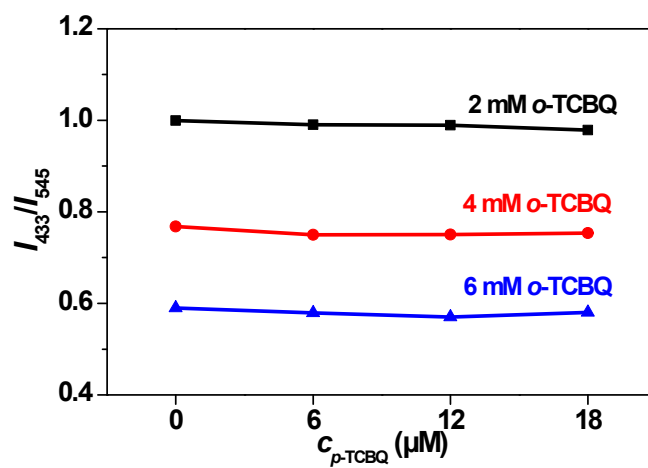


Fig. S10 Effect of *p*-TCBQ on the ratiometric fluorescent signal induced by *o*-TCBQ, $\lambda_{\text{ex}} = 290$ nm.

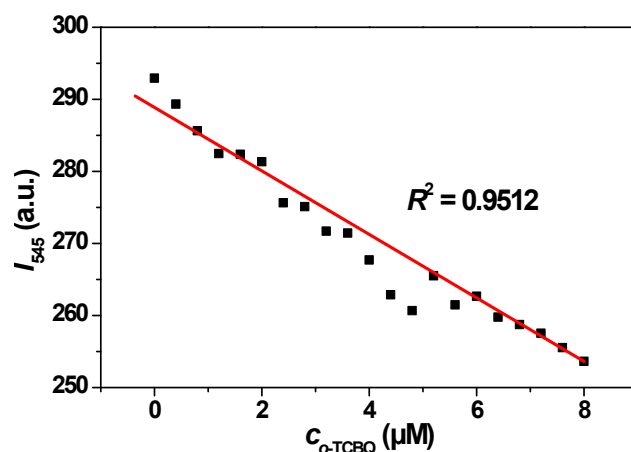


Fig. S11 Linear fitting of the intensity change of Tb@UiO-66-(COOH)₂NH₂-40 at 545 nm with the addition of different concentrations of *o*-TCBQ.

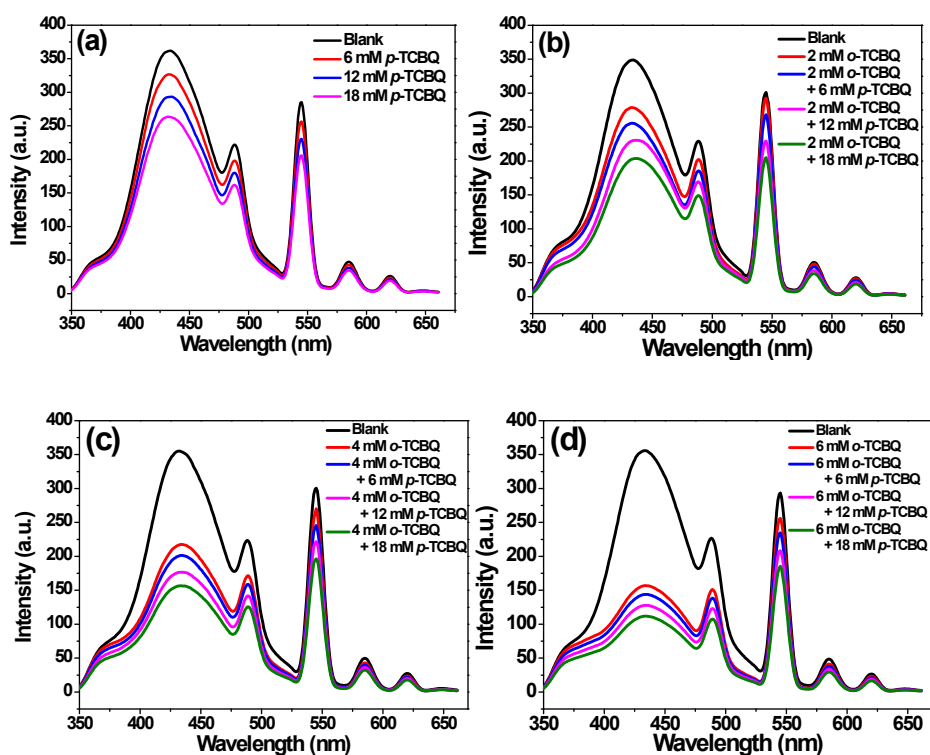


Fig. S12 The photoluminescent spectra of Tb@UiO-66-COOH₂NH₂-40 (50 mg L⁻¹) in the mixed solutions of *o*- and *p*-TCBQs, $\lambda_{\text{ex}} = 290$ nm.

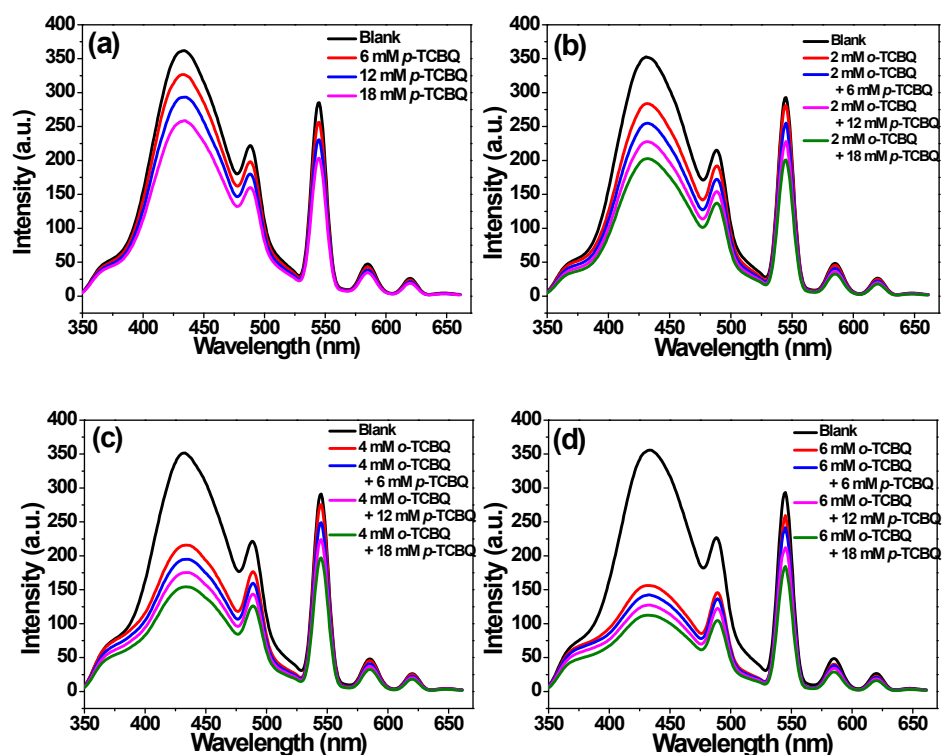


Fig. S13 The photoluminescent spectra of Tb@UiO-66-COOH₂NH₂-40 (50 mg L⁻¹) in artificial urine under the addition of different concentrations of *o*- and *p*-TCBQs, $\lambda_{\text{ex}} = 290$ nm.

Table S1 The ICP-OES results of Tb@UiO-66-(COOH)₂NH₂-40 before and after detection experiment

Material	Zr (Wt%)	Tb (Wt%)	Molecular ratio Zr:Tb
As-prepared	13.7	4.82	2.84:1
After <i>o</i> -TCBQ detection	11.36	4.04	2.81:1
After <i>p</i> -TCBQ detection	12.90	4.62	2.79:1